Absolute Density Calibration Cell for Laser Induced Fluorescence Erosion Rate Measurements

Matthew T. Domonkos
NASA John H. Glenn Research Center
Mail Stop 301-3
21000 Brookpark Road
Cleveland, Ohio 44135
216-433-2164
Matthew.T.Domonkos@grc.nasa.gov

Richard E. Stevens
Whitworth College
Spokane, Washington

IEPC-01-300[*]

Abstract

Flight qualification of ion thrusters typically requires testing on the order of 10,000 hours. Extensive knowledge of wear mechanisms and rates is necessary to establish design confidence prior to long duration tests. Consequently, real-time erosion rate measurements offer the potential both to reduce development costs and to enhance knowledge of the dependency of component wear on operating conditions. Several previous studies have used laser-induced fluorescence (LIF) to measure real-time, *in situ* erosion rates of ion thruster accelerator grids. Those studies provided only relative measurements of the erosion rate. In the present investigation, a molybdenum tube was resistively heated such that the evaporation rate yielded densities within the tube on the order of those expected from accelerator grid erosion. This work examines the suitability of the density cell as an absolute calibration source for LIF measurements, and the intrinsic error was evaluated.

Nomenclature

a,b,c,d = coefficients for vapor pressure calculation
A = view factor variable
A_i, A_j = surface area of i or j, m^2
dx = width of element i
d_e = diameter of surface j
d_x = diameter of element i
F_{i-j} = view factor between i and j
F_{dx-e} = differential view factor between dx and e in cylindrical geometry
j_{evap} = evaporative flux, m^{-2}s^{-1}

k = Boltzmann's constant, 1.38 x 10^{-23} J/K
m = mass of vapor, kg
n = number density, m^{-3}
p_v = vapor pressure, Pa
T = temperature, K
$\bar{v}$ = mean velocity, m/s
$\bar{v}_i$ = mean vapor velocity from i, m/s
$\bar{v}_{n,j}$ = mean vapor velocity normal to j, m/s
x = distance between i and j, m

IEPC-01-300 27th International Electric Propulsion Conference

Introduction

At the NASA Glenn Research Center (GRC), a real-time, *in situ* erosion diagnostic for ion thrusters is currently under development using laser induced fluorescence (LIF).[1] The low thrust (<500-mN) of all flight demonstrated electric rockets necessitates long life (1,000 to greater than 10,000 hours) to conduct orbit transfer or planetary missions. At a minimum, flight qualification requires thruster operation at the maximum wear condition for a sufficient duration to conduct the desired mission and is therefore costly and time consuming. A real-time, *in situ* erosion rate measurement will enable both calculation of the dependence of component life on operating conditions and determination of the true maximum wear condition without the need for long-duration tests.

By tuning a laser to a ground state transition of the eroding species, LIF has been used to detect sputtered molybdenum downstream of the accelerator grid.[2,3,4] Under typical discharge chamber and beam plasma conditions, the vast majority of the sputtered atoms are in the ground state, and interrogation of this population yields the most representative measure of the species density. The works by Gaetta, et al.[2,3] and Crofton[4] neglected calibration of the LIF signal, and consequently their results can only be interpreted as relative rates. By controlling the evaporation rate of the target species, the LIF density diagnostic can be calibrated using a known density source. Evaporation of the target species can be controlled with a high degree of precision by resistively heating a tube of the same material as the target component. This paper reports the ongoing efforts at NASA GRC to develop a calibration cell for LIF absolute density measurements.

Previous works[2,3,4] have sought to provide a real-time *in situ* erosion rate measurement using LIF. Several difficulties associated with implementation have so far prevented the use of the diagnostic for practical measurements. Gaetta et al.[2,3] were able to detect molybdenum downstream of the accelerator grid of an ion engine at voltages between 200 and 600-V below ground. The work focused on ground state resonant fluorescence at 390.2-nm in molybdenum. Gaetta et al.[2,3] used a CW tunable dye laser pumped by an argon ion laser, and the collection of the fluorescence was accomplished using a lens and a monochromator. The maximum intensity of the laser and any discussion of saturation were absent from these works.[2] Crofton[4] performed a similar study of accelerator grid erosion also using resonant fluorescence of the 390.2-nm line with a maximum laser power of 20-mW. The study demonstrated relative density detection of molybdenum downstream of the thruster for accelerator grid voltages between 225 and 350-V below ground. Additionally, relative sensitivities to beam current and propellant utilization efficiency were also reported.[4] An alternate molybdenum transition was employed by Orsitto, et al.[5] to detect molybdenum in a tokomak plasma. Non-resonant fluorescence of the ground state at 345.64-nm was used, with the fluorescence at 550.6-nm.[5] The work by Orsitto, et al.[5] demonstrated absolute density detection capability down to 2.5×10^{14} m^{-3}. The calibration was accomplished by both measuring the laser bandwidth and intensity and calibrating the collection optics. The laser system consisted of a dye laser pumped by an excimer laser with a peak pulse energy of approximately 320-μJ in a 10-ns pulse with a bandwidth of 4-pm. The collection optics consisted of a lens, a 2.52-nm bandwidth interference filter and photomultiplier tube which were calibrated using a standard spectral radiance lamp. The use of non-resonant fluorescence greatly simplifies the collection optics, and the interference filter generally enables greater sensitivity to the fluorescence than a monochromator. Additionally, the threshold density for molybdenum detection in the relatively quiescent ion thruster environment is expected to be lower due to the low plasma temperatures and absence of the Zeeman effect.

In 1999, work was initiated at the NASA Glenn Research Center to develop a real-time, *in situ* erosion rate diagnostic using LIF, and this paper reports the progress on the creation of a calibration cell for the LIF diagnostic. The theory behind the calibration cell is discussed, followed by a description of the experimental apparatus. Next, the experiments conducted to date and their results are presented. The experimental results are discussed as is the overall error expected with this technique. Finally the major conclusions of this work are summarized.

Theory

Absolute calibration of a laser-induced fluorescence density measurement can be accomplished either by measuring a known density of the target species or by careful calibration of the collection optics. The latter technique requires a spectral radiance lamp standard. Spectral radiance lamps are insufficiently robust to be employed in an *in situ* calibration capacity. Conversely, a density cell made of the target species is relatively easy to implement since the calibration cell is more resistant to the near thruster environment than a spectral radiance lamp. Consequently, a density standard was adopted to calibrate the LIF erosion diagnostic. The remainder of this section presents the development of a model to describe the calibration cell.

The density within the reference cell is calculated based upon vapor pressure data for the target material. By definition, the vapor pressure, p_v, is the equilibrium pressure in an enclosed volume with uniform temperature. Reference data exist for the dependence of the vapor pressure on temperature, and Figure presents data for molybdenum in the range of interest.[6,7,8,9,10] The curves in Figure were calculated from the general formula

$$p_v = 101,325 * 10^{\left(a + \frac{b}{T} + c \log T + dT\right)}$$ (1)

where the constants a, b, c, and d are tabulated for many elements in Reference [7]. From the pressure and temperature, the number density can be calculated from the ideal gas law. Based on the accelerator grid erosion observed in the 8,200 hour wear test, a molybdenum reference cell would have a temperature of 1962-K under ideal conditions to replicate the density of eroded atoms downstream of the accelerator grid on centerline, 5×10^{14}-m^{-3}.[1,11] Departure from the idealized vapor pressure cell occurs when considering open systems with non-uniform temperature.

The practical considerations for the application of an LIF density calibration cell dictate the use of an open geometry; optical access is required for the laser, the fluorescence detection, and the temperature measurement. Additionally, heating the target material to the temperature required for calibration while minimizing apparatus size led to a resistively heated design. Consequently temperature non-uniformities must be considered when determining the density distribution of vapor atoms. Both largely and minimally open configurations are considered here. The largely open configuration can be either a wire or thin strip of molybdenum. Optical access for LIF is maximized. The drawback of the open geometry is that the density of vapor atoms is highly dependent upon location and may vary significantly across the beam diameter. Nevertheless, the variation of density with position enables an alternate means to calibrate over a range of density. While the temperature and density distribution around a wire or a flat strip are straightforward to calculate, the position, diameter, and distribution of the laser must be well known to yield an accurate measurement. Since the pressure and density above a pure phase with uniform temperature within an enclosed volume are accurately described by the vapor pressure, the error introduced by laser shape and location is minimized by using an enclosure with the necessary optical access. A long tube of pure molybdenum was chosen as a convenient, semi-enclosed reference cell. A hollow cylinder with open ends approaches the enclosed geometry when the length is much greater than the diameter. Resistively heating the cylinder results in a non-uniform axial temperature distribution. Consequently, implementation of this calibration technique requires modeling to account for the departure of the experimental apparatus from the idealization.

Density Distributions

To begin the calculation of the density distribution within the calibration cell, the evaporation rate based on the temperature and vapor pressure is evaluated. By equating the evaporative flux to the incoming isotropic flux (the equilibrium condition assumed when determining the vapor pressure)

$$j_{evap} = j_{in}$$ (2)

the evaporation rate is

$$j_{evap} = \frac{1}{4} n \bar{v} = \frac{p_v}{4kT} \sqrt{\frac{8kT}{\pi m}}$$ (3)

Since resistive heating of the calibration cell results in a non-uniform temperature distribution, the evaporation rate must be calculated for differential elements, i, along the surface. Figure 1 depicts the schematic of the cylindrical geometry for modeling purposes. The vapor flow is free molecular, and the assumption of isotropic evaporation from the surface enables the uses of geometric view factors in a straightforward manner to determine the vapor flux at

a virtual surface j from each of the differential elements i. The normal component of the vapor velocity for the flux arriving at surface j from element i has a small distribution when the diameter of j is small. Under this criterion, the velocity component of the vapor from i that is normal to j can be approximated as

$$\overline{v}_{n,j} = \overline{v}_i \frac{x}{\sqrt{x^2 + \dfrac{d_x^2}{4}}} \qquad (4)$$

By applying conservation of mass at the surface j for each element i, the number density at j due to the flux from element i is

$$n_{j,i} = \frac{1}{4} \frac{\sqrt{x^2 + \dfrac{d_x^2}{4}}}{x} n_i F_{i-j} \frac{A_i}{A_j}. \qquad (5)$$

The total density at surface j is then the sum of the densities due to each element i.

$$n_j = \sum_i n_{j,i} \qquad (6)$$

This technique was used to simplify the analysis of the variation of vapor density in or around a calibration cell. The simplified analysis also facilitates estimation of errors inherent to the calibration cell. For cosine or other distributions of the vapor flux from the surface, new view factors and flux equations must be used.

Density Distribution Within a Cylinder

While an open geometry simplifies the prediction of the density distribution, the physical limitations on beam diameter make the use of a cylinder for the calibration cell more attractive because the geometry yields more gentle density gradients. Consequently, the detailed analysis for the cylindrical geometry is presented here. Equations 5 and 6 may be used with the appropriate view factors for any other geometry. The view factors for the cylindrical geometry were taken from Van Noord.[12] The view factor between a differential element of negligible width (dx) of the cylinder and a virtual circular surface normal to the cylinder surface is

$$F_{dx-e}(x) = \left[\frac{A}{\left(A^2 - \dfrac{d_e^2 d_x^2}{4} \right)^{1/2}} - 1 \right] \frac{x}{d_x} \qquad (7)$$

where

$$A = x^2 + \frac{d_e^2 + d_x^2}{4} \qquad (8)$$

The definition of the geometric terms is given in Figure 1. The diameter and position of the circular surface can be varied to calculate the number density distribution within the calibration cell. Therefore, the number density can be determined for an arbitrary beam diameter and interrogation location.

Apparatus

The experimental set-up is shown in Figure 2. The molybdenum tube was made by rolling a sheet 7.6 x 10^{-2}-mm thick into a 6.4-mm diameter cylinder. The tube is 85-mm long between the clamps, which add 13-mm to the overall length. The tube has a 3.2-mm diameter hole at the tube center that is used to collect the fluorescence and for optical temperature measurements. A DC-regulated power supply which is governed to approximately 126-A maximum is used to power the reference cell. Four type R thermocouples were used to measure the external, axial temperature distribution. The location of the thermocouples is depicted in Figure 3. They were spot welded and strapped to the molybdenum tube to ensure minimal thermal contact resistance.

A schematic of the pulsed laser system used in this investigation is presented in Figure 4. A Nd:YAG laser pumps a dye laser with the 532-nm second harmonic. The dye laser was operated with the LDS-698 dye with a maximum output of 60-mJ/pulse. The dye laser was tuned to approximately 690-nm, and the output was sent to a BBO crystal where second harmonic generation yielded the desired 345.64-nm beam. Part of the ultraviolet beam was sampled by a pulsed wavemeter to assist in tuning the laser. The second harmonic has been demonstrated up to 1.5 mJ/pulse with new dye. The beam was coupled into a 0.6-mm diameter core fused silica fiber optic for delivery to the vacuum chamber. This means of beam delivery provides the flexibility necessary for varied operations in VF-11 at the NASA Glenn Research Center, however, the maximum demonstrated pulse energy out of the fiber was approximately 350-μJ, indicating strong attenuation. Nevertheless, 350-μJ for this transition in molybdenum has been demonstrated to be sufficient for detection of number densities as low as 2.5 x

10^{14} m^{-3}.[5] Increased density detection sensitivity may be achieved with the existing system either by more direct application of the laser to the interrogation region or by stronger collection optics. Several lenses and ultraviolet laser mirrors were used to collimate the beam through the calibration cell, as illustrated in Figure 2.

The optical system was configured to detect fluorescence using an intensified CCD (ICCD) camera with an interference filter. The filter is centered at 550-nm with a 10-nm bandpass. A simple lens was used to collect the fluorescence signal. A TTL signal from the Q-switch was used to trigger the ICCD electronics for data acquisition. Additionally, a photodiode was used to detect the intensity of the laser after it had passed through the calibration cell. While the laser passed through a fused silica window prior to being collected in the photodiode, this loss was considered much smaller than those experienced in the beam delivery system.

Analysis and Discussion of the Calibration Cell

The initial experiments with the calibration cell focused on obtaining the desired temperature and accurately determining the temperature distribution. The external tube temperature distributions for the apparatus described in Figure 3 are presented in Figure 5 for several different currents. The strong axial temperature gradients necessitate detailed analysis of the number density distributions within the calibration cell. Only the external temperatures were measured here to assess the temperature gradient. The measurements in Figure 5 indicate that the calibration cell internal temperature distribution must be measured to yield accurate knowledge of the density distribution within the tube. Internal thermocouples will be incorporated into future iterations of the cylindrical geometry of the calibration cell.

Figure 5 also presents the evaporation rate of molybdenum along the cell. Along the length, the evaporation rate varies by over an order of magnitude. Consequently the surface density of molybdenum vapor varies over a similar range. In order to estimate the radial variation of the number density, the internal temperature distribution was assumed to be equivalent to the measured external temperatures. This approximation was made only to assess the relative radial distribution of molybdenum vapor number density within the cell. The resulting distribution of molybdenum vapor calculated using Equations 4, 5 and 6 for the 126-A case is presented in Figure 6. In the contour plot, 45-mm is the center of the tube, and axial symmetry is assumed about this point. Figure 6 illustrates that the radial variation of number density, though more gentle than the axial variation, is nonetheless considerable and must be calculated to minimize the error associated with the proposed calibration technique. The ability to calculate the full spatial distribution of the number density within the cell enhances the accuracy of the calibration technique.

The error associated with this calibration technique was also assessed to evaluate its merit. The error in the surface number density for several temperature errors is presented in Figure 7. The temperature must be known to within a few Kelvins in order for the calibration cell to be considered useful. Error analysis of the density at the cylinder center point in Figure 6 was also performed using a Monte Carlo technique to model the temperature and pressure errors as normal distributions. The error in the vapor pressure was reported to be less than five percent [7] which was interpreted as the standard deviation on a normal distribution. The results of the analysis are presented in Table 1. Even for a relatively small error in the temperature measurement, the calculated density is accurate to 22 percent with a 95 percent degree of confidence. Note that the errors presented in Table 1 are skewed toward values greater than the true average number density; the analysis precludes calculation of number densities substantially below the true average.

The error associated with the calibration technique can be reduced from the case presented by incorporating any of several modifications. By increasing the length of the calibration cell, the axial variation of temperature, and thereby density, near the center can be reduced. Additionally the thickness of the molybdenum used in the calibration cell can be reduced to support a larger temperature gradient near the clamps. Finally, a more rigorous analysis of the vapor transport within the tube using a gaskinetic theory model would also yield a more accurate cell. The effect of the analysis technique was omitted from the error assessment in this paper.

Future Work

In addition to improving the accuracy of the cell in future iterations, laser induced fluorescence detection of the molybdenum vapor must be demonstrated, and the sensitivity of the LIF diagnostic to changes in vapor density must be assessed to evaluate the effectiveness of the calibration technique. These tasks are planned for near term implementation at the NASA Glenn Research Center.

Conclusions

A calibration cell for the absolute density of metal vapors was presented. The cell will be used to calibrate a laser induced fluorescence diagnostic to measure the sputter rate of ion thruster components. The basic theory of the calibration cell was presented. A simplified analysis technique was reported to calculate the vapor density within the cell. To date, an experimental cell has been constructed, and the details of the apparatus were discussed. The experimental cell has been operated near the regime necessary to produce densities comparable to those expected from accelerator grid erosion at the NSTAR full power condition. The temperature distribution in the experimental cell was used to calculate the density variation in the cell and the error associated with the predicted value. Some techniques to improve the accuracy were discussed.

References

[1] M. T. Domonkos and G. J. Williams, "Status of Laser Based Ion Engine Diagnostics at NASA Glenn Research Center," IEPC Paper No. 2001-304, International Electric Propulsion Conference, Pasadena, CA, Oct. 2001.

[2] C. J. Gaetta, et al., "Plasma Erosion-rate Diagnostics Using Laser-Induced Fluorescence," *Review of Scientific Instruments*, Vol. 63, No. 5, May 1992, pp. 3090-3095.

[3] C. J. Gaetta, "Erosion Rate Diagnostic in Ion Thrusters Using Laser-Induced Fluorescence," *Journal of Propulsion and Power*, Vol. 9, No. 3, May-June 1993, pp.369-376.

[4] M. W. Crofton, "Laser Spectroscopic Study of the T5 Ion Thruster," AIAA Paper 95-2921, *31st AIAA / ASME / SAE / ASEE Joint Propulsion Conference*, San Diego, CA, July 1995.

[5] F. Orsitto, et al., "MoI Density Measurements by Laser Induced Fluorescence Spectroscopy," *Review of Scientific Instruments,* Vol. 70, No. 1, Jan. 1999, pp. 921-924.

[6] *CRC Handbook of Chemistry and Physics, 81st Edition,* D. R. Lide, Editor in Chief, CRC Press, Boca Raton, 2000.

[7] C. B. Alcock, V. P. Itkin, and M. K. Horrigan, "Vapour Pressure Equations for the Metallic Elements: 298-2500K," *Canadian Metallurgical Quarterly,* Vol. 23, No. 3, pp. 309-313, 1984.

[8] *Molybdenum Metal*, CSM Industries, 1960.

[9] *ASM Handbook: Volume 4 Heat Treating*, edited by S. R. Lampman, T. B. Zorc, J. L. Daquila, and A. W. Ronke, ASM International, United States, 1991.

[10] A. N. Nesmeyanov, *Vapour Pressure of the Elements*, Academic Press, New York, 1963.

[11] J. E. Polk, et al., "An Overview of the Results from an 8200 Hour Wear Test of the NSTAR Ion Thruster," AIAA Paper No. 99-2446, *35th AIAA / ASME / SAE / ASEE Joint Propulsion Conference*, Los Angeles, CA, June 1999.

[12] J. L. Van Noord, "Thermal Modeling of an Ion Thruster," NASA/CR 2000-209792, February 2000.

Table 1 - Calculated Sensitivity of Number Density Error to Error in the Temperature Measurements for Tube Geometry Results in Figure 6.

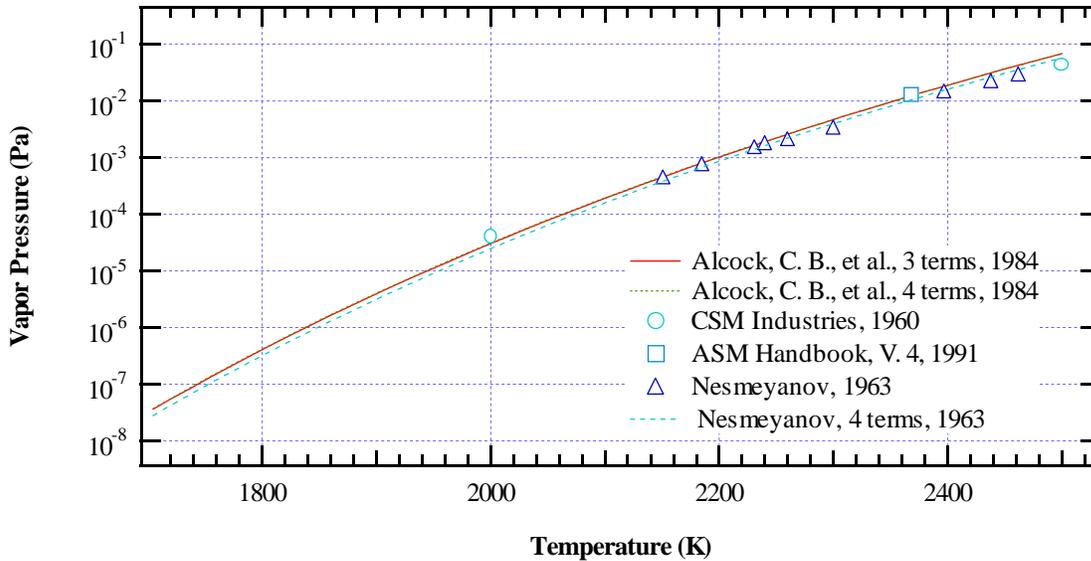| Standard Deviation of Temperature (K)	Percentage Error in Density to >95% Confidence
5	22
10	45
25	125
50	311

Figure - Vapor Pressure of Molybdenum in the Region of Interest.[6,7,8,9,10]
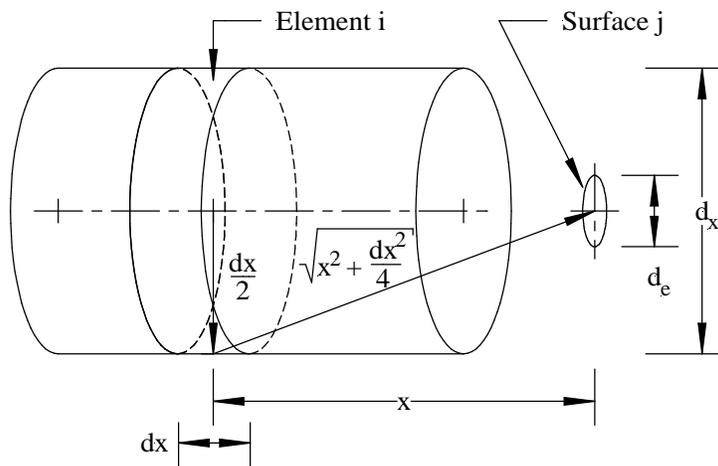
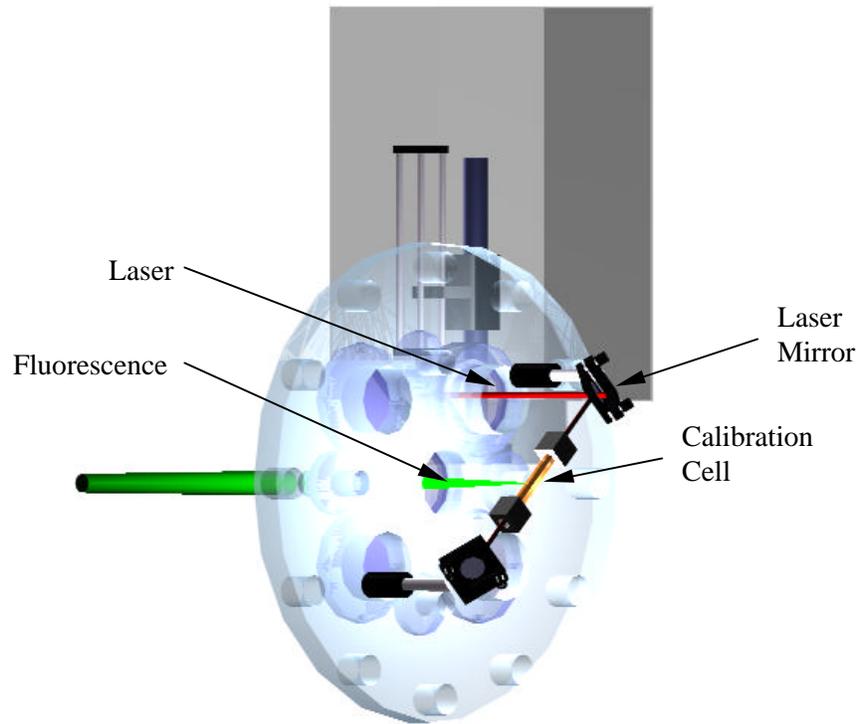**Figure 1 – Cylindrical Calibration Cell Schematic Used to Calculate Densities.**

Figure 2 - Schematic of the Calibration Cell Showing Laser in Red and the Fluorescence Signal in Green.

39.8   26.2   13.7   1.3

Clamp Ends
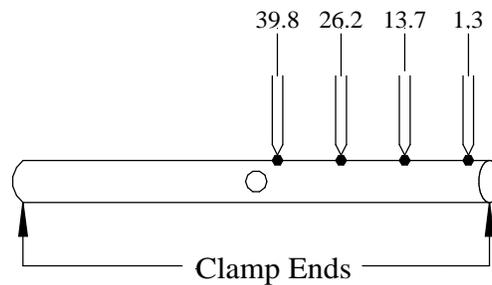
Figure 3 - Description of Thermocouple Locations on Calibration Cell Tube. Dimensions in mm.
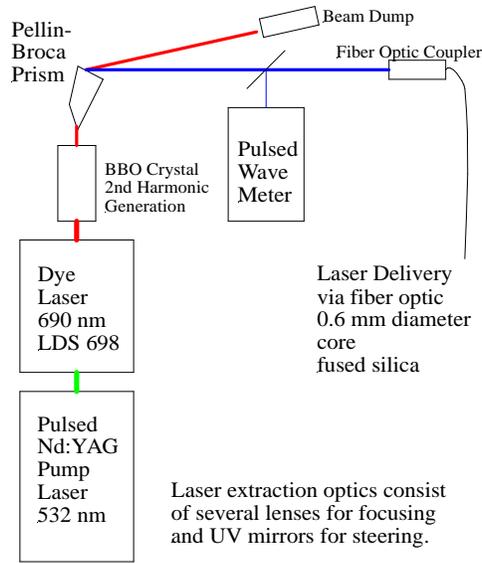
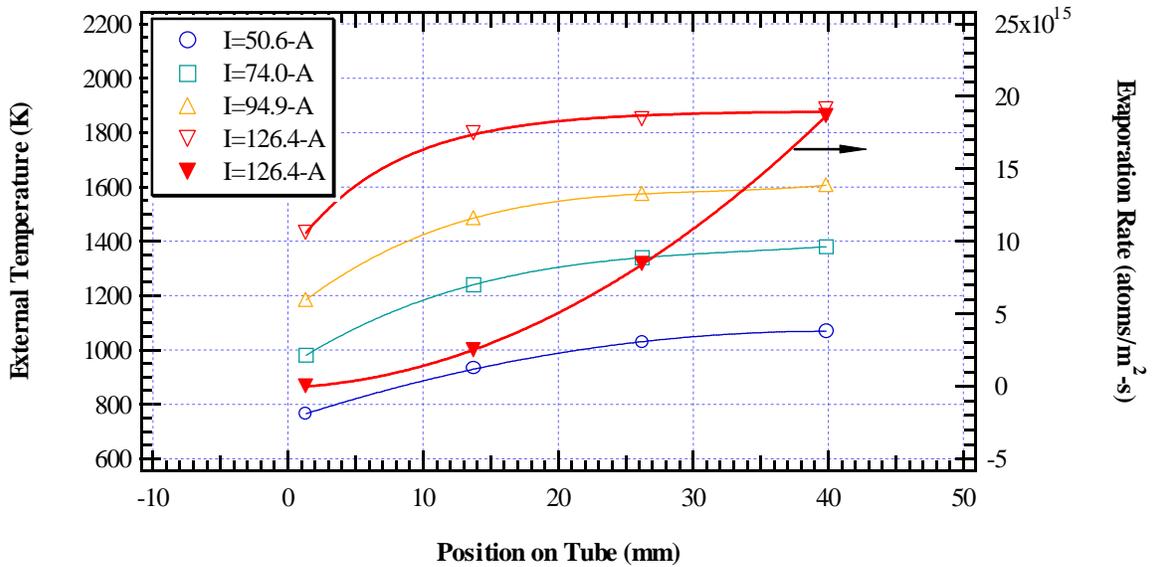**Figure 4 - Schematic of the Pulsed Laser System.**

Figure 5 - Measured External Temperature Distribution for the Molybdenum Tube.
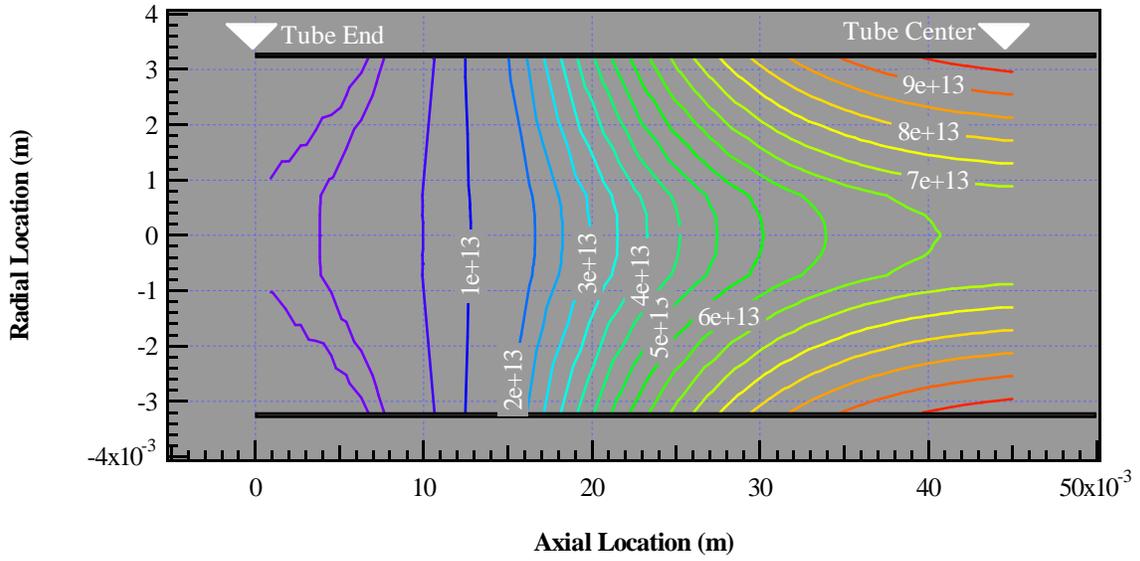
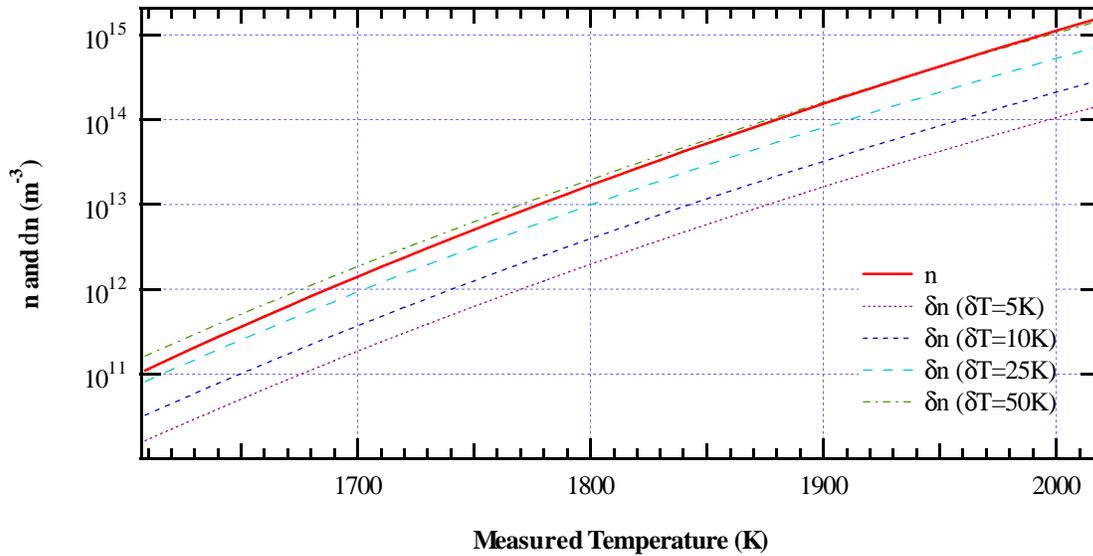**Figure 6 - Calculated Molybdenum Number Density Within Calibration Cell at 126-A.**

Figure 7 - Error Induced in the Surface Density by Error in the Temperature Measurement.